EuroCC@Turkiye

This document is prepared by EuroCC@Turkey for EuroCC 2 under GA NO 101101903

Mechanistic Insights Into the [2+2] Cycloaddition-Retroelectrocyclization Reactions of Symmetric Alkynes Activated with Methoxy Groups

1. Problem Identification

[2+2] Cycloaddition-retroelectrocyclization (CA-RE) represents reactions that occur between electron-rich alkynes and electron-deficient alkenes (Scheme 1).[1]

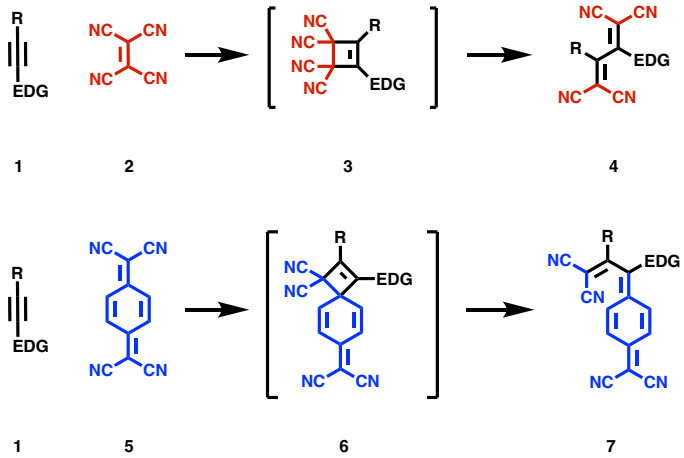

Scheme 1. [2+2] CA-RE reactions between electron-rich alkynes and electron-deficient alkenes.

Bruce and co-workers reported the first reactions between metal-substituted acetylides and an electron-deficient olefin back in 1981.[2] Until 2005, these reactions were reported with transition metal-substituted alkynes. However, Diederich and his research group showed that [2+2] CA-RE reactions can be applied with organic alkynes as well.[3] According to the Woodward-Hoffman rules, [2+2] reactions are thermally forbidden yet surprisingly occur at a high yield at room temperature.[4] There are commercially available electron-poor alkenes that can be used in these reactions such as tetracynanoethylene, TCNE (**2**)[5] and tetracyanoquinodimethane, TCNQ (**5**)[6].

In this study, four new electron-rich alkynes were synthesized starting from 1,4-dimethoxybenzene **8**. Then, Sonagashira cross-coupling reaction of **9** was applied with different acetylenes **10-13** which gave the alkynes **14-17**. Treatment of **14-17** with TCNE yielded different products shown in Scheme 2. While the reaction of **14** with TCNE was carried out at room temperature, the reactions of **15-17** with TCNE were carried out at 82 °C.

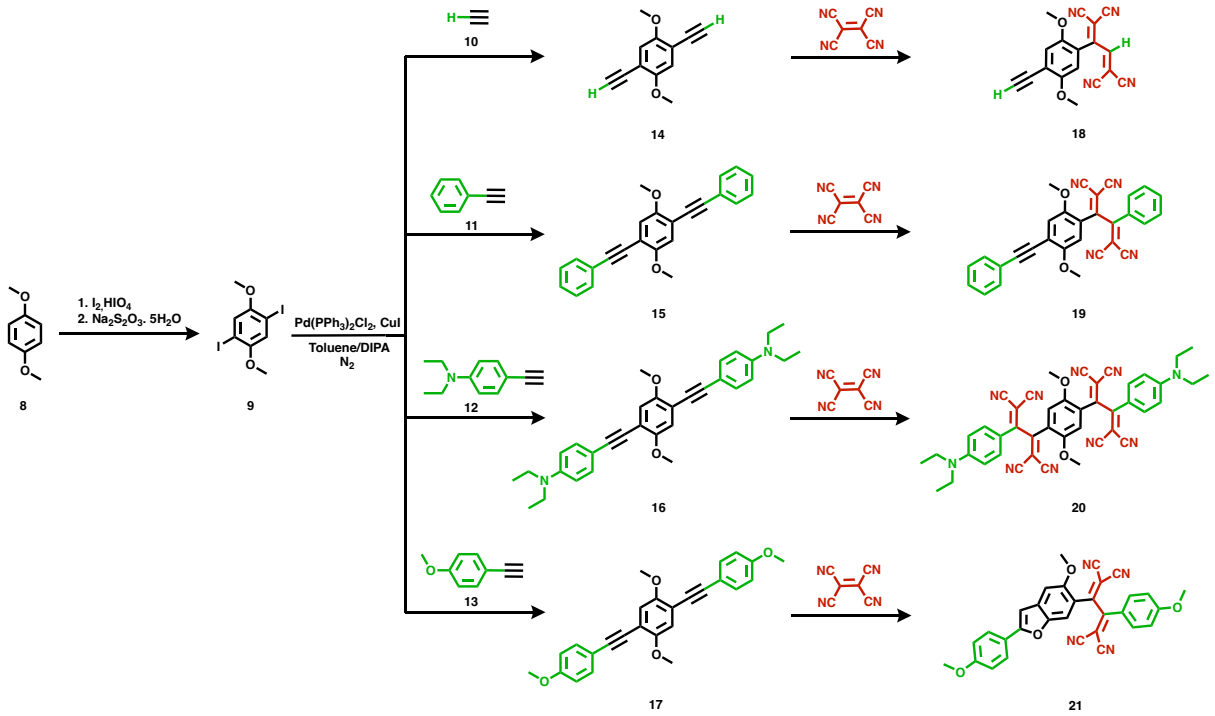

Scheme 2. [2+2] CA-RE reaction of selected alkynes.

The purpose of this study is to explore the [2+2] CA-RE reactions between TCNE with corresponding alkynes (**10-13**) having different electron densities. In the case of **14** and **15**, the addition takes place from only one alkyne moiety producing chromophores **18** and **19**, while in **16**, the addition takes place from both alkyne moieties resulting in the formation of chromophore **20.** In the case of compound **17**, a notably interesting cyclization product was observed.

To understand the main factors causing these differences in reactivity, the reaction should be examined by means of theoretical calculations. Since Dengiz's research group specializes in experimental studies, an academic and infrastructure expert with experience in the field of computational organic chemistry to provide guidance to rationalize the experimental observations was requested. In this PoC, the NCC expert mentored a graduate student who is working experimentally but is enthusiastic about theoretical modeling.

The tentative project plan is as follows:

Timeline	Tasks and Milestones
Months 1-2	A brief introduction to computational organic chemistry and reaction modeling: Schrödinger equation, wave functions and molecular orbitals, reaction pathways, thermodynamics, Hartree-Fock theory, basis sets, semiempirical methods, Density Functional Theory (DFT), Potential energy profiles
Month 3	Learning and using computational software packages - Gaussian Program Package for calculations and GaussView for Graphical User Interface (GUI)
Month 4-5	Employing the computational tools (Gaussian and GaussView) for visualization of the structure, geometry optimization, location of local and global minima and transition states, vibrational frequency analysis, Intrinsic Reaction Coordinate (IRC) analysis, free energy calculations, Single Point Energy (SPE) calculations Basic Linux Commands Learning how to use MobaXterm Learning how to submit a job on HPC infrastructure (TRUBA) Analyzing the results from the output file
Months 6-11	Mechanistic studies on the [2+2] CA-RE reactions, modeling the transition states for [2+2] CA-RE reactions and calculating free energy values. Drawing potential energy profiles
Month 11-12	Identifying the most plausible reaction mechanism

2. Results and Achievements

2.1. Mechanistical Studies for [2+2] CA-RE Reaction

The mechanism for [2+2] CA-RE reactions are still under investigation. In 1981, Bruce and co-workers successfully isolated the intermediate cyclobutadiene structure, proposing that the reaction follows a concerted mechanism.[2] In 2022, Hansen and co-workers suggested that the mechanism is autocatalytic and could proceed through a non-concerted mechanism.[7] In our studies, we first suggested that the mechanism follows a non-concerted mechanism (Scheme 3). The first step is the nucleophilic attack of the alkyne moiety to the TCNE molecule forming a zwitterionic intermediate **I1**. This intermediate then undergoes ring closure leading to cyclobutadiene intermediate **I2**. Subsequently, ring opening (retro electro cyclization) occurs and yielding the final product **P3**.

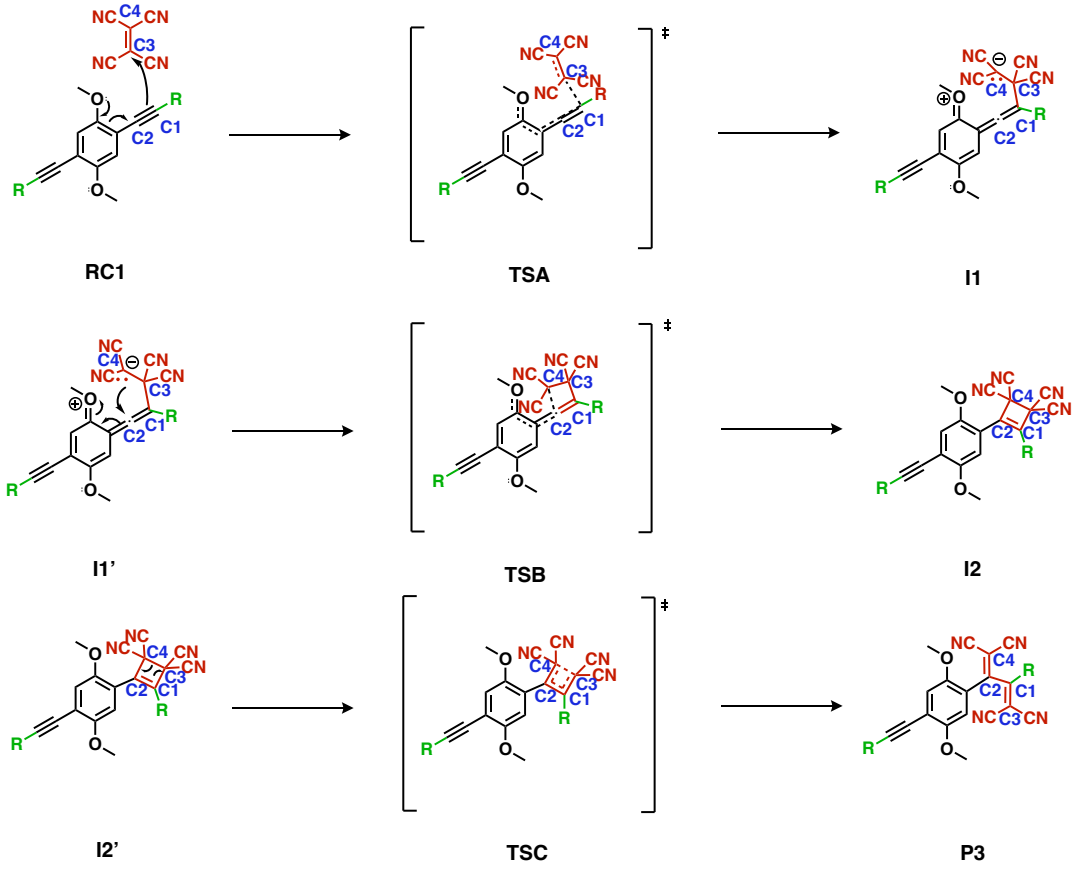

Scheme 3. Proposed non-concerted mechanism for [2+2] CA-RE reaction.

However, Intrinsic Reaction Coordinate (IRC) calculations revealed that the formation of cyclic intermediate **I2** occurs asynchronous concerted pathway. As shown in Figure 1, the bond formation between C1 of the alkyne fragment and C3 of TCNE is almost complete before the bond formation between C2 of the alkyne and C4 of TCNE occurs.

For the formation of **P3**, the C1-C3 distance decreases from 2.79 Å in **IRC41** to 1.73 Å in **TS1'** (Figure 1) while the C2-C4 distance decreases from 2.86 Å in **TS1'** to 2.00 Å in **IRC-1** (Figure 1). It should be noted that **IRC-1** and **IRC-41** are not the product and reactant, but rather the 1st and 41st points on the IRC. These findings indicate asynchronous events.

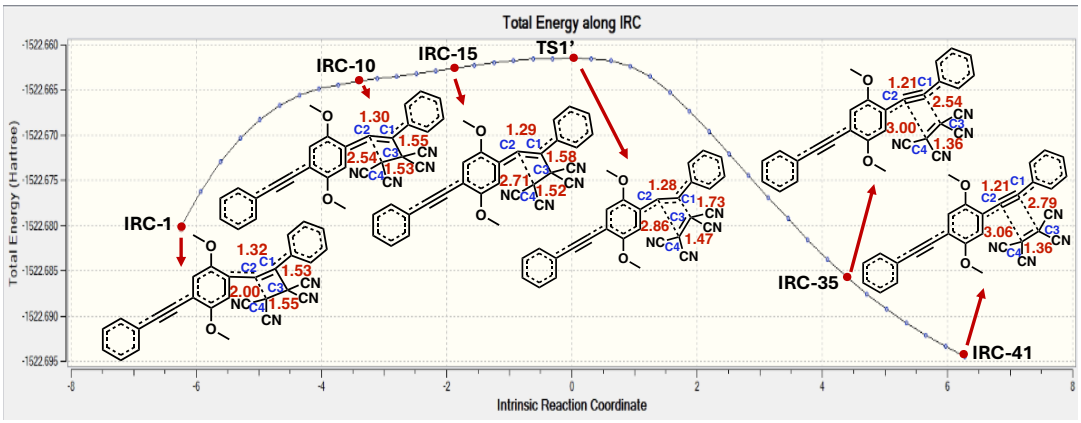

Figure 1. IRC calculated for the formation of phenylacetylene substituted TCBD **(13)** at M06-2X/6-31+G(d,p) level. **IRC-1**, **IRC-15**, **IRC-35**, **IRC-41**, etc. are the selected points along the coordinate. Distances (red) are given in Å.

In line with these observations, the following reaction mechanism has been proposed for [2+2] CA-RE reactions (Scheme 4).

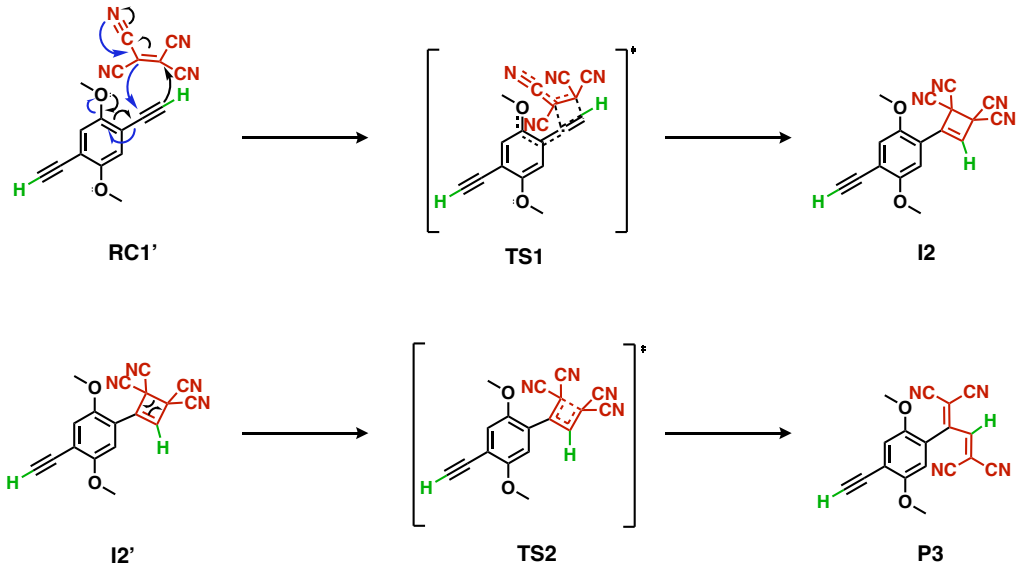

Scheme 4. Proposed mechanism for [2+2] CA-RE reaction.

2.2. [2+2] CA-RE Reaction of Acetylene Substituted Alkyne (14)

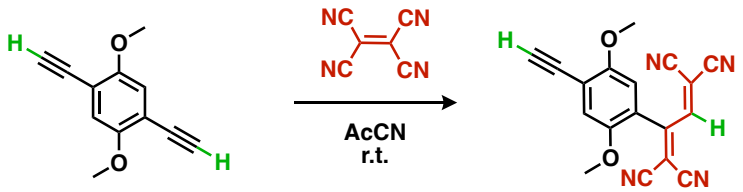

14 **18 (60%)**

Scheme 5. [2+2] CA-RE reaction of **14** with TCNE.

The optimized geometries and potential energy profile of the stationary points for the formation of **P3** is shown in Figure 2-4. The calculated free energy of activations was found to be 20.4 kcal/mol and 4.6 kcal/mol with respect to **RC1'**. The overall reaction is quite exergonic by 34.7 kcal/mol relative to **RC1'.**

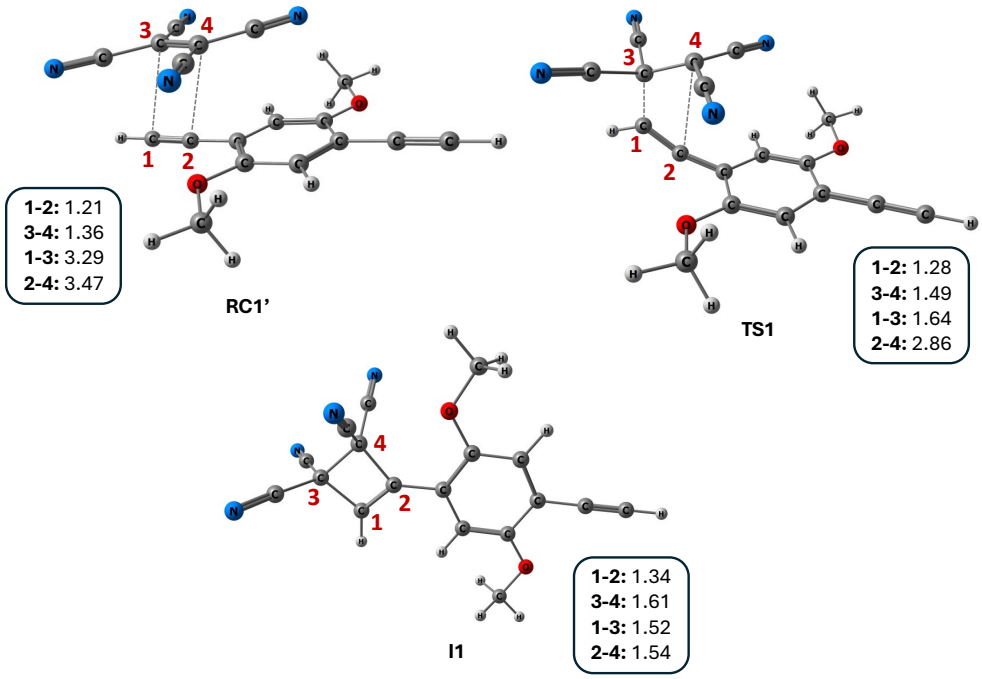

Figure 2. Optimized geometries of the stationary points **RC1'**, **TS1** and **I1** at PCM/M06-2X/6-311++G(d,p)//M06-2X/6-31+G(d,p) level in acetonitrile. Distances are given in Å.

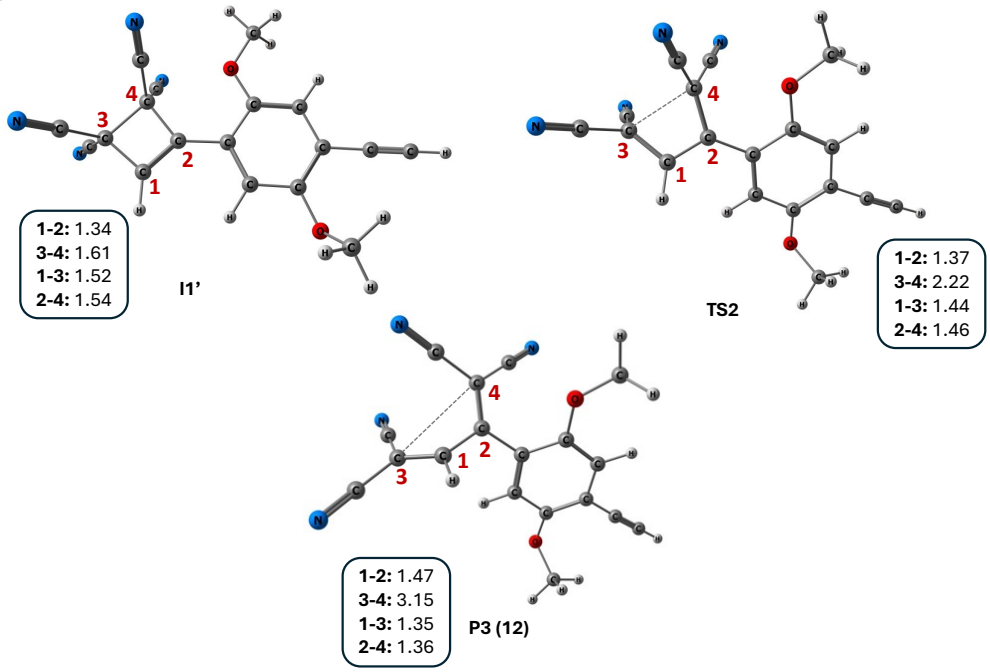

Figure 3. Optimized geometries of the stationary points **I1'**, **TS2** and **P3 (12)** at PCM/M06-2X/6-311++G(d,p)//M06-2X/6-31+G(d,p) level in acetonitrile. Distances are given in Å.

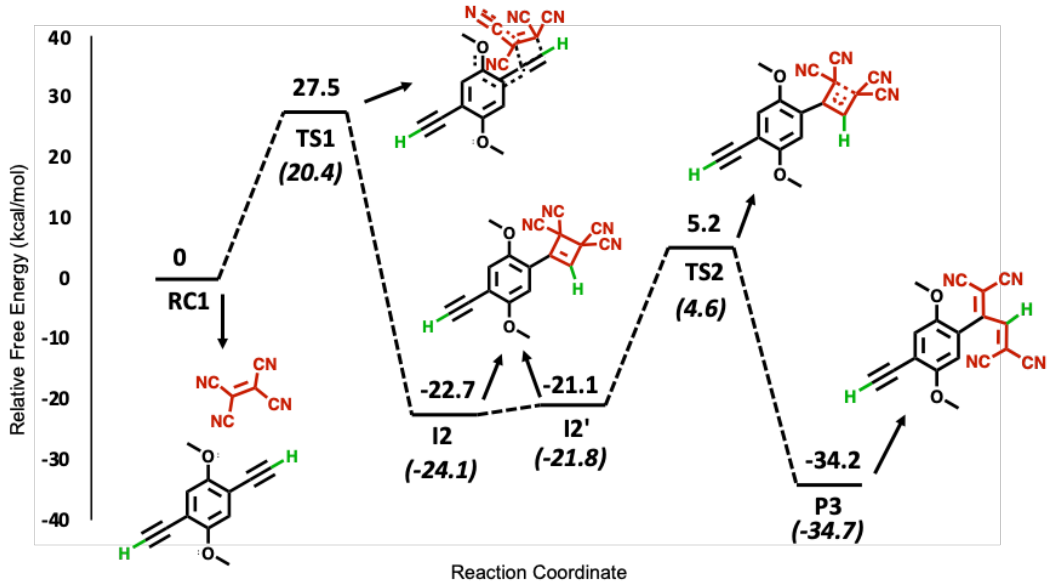

Figure 4. Potential energy profile for the formation of **P3** at PCM/M06-2X/6-311G++(d,p)//M06-2X/6-31G+(d,p) level in acetonitrile. Energy values in parenthesis are solvent energies.

2.3. [2+2] CA-RE Reaction of Phenyl Substituted Alkyne (15)

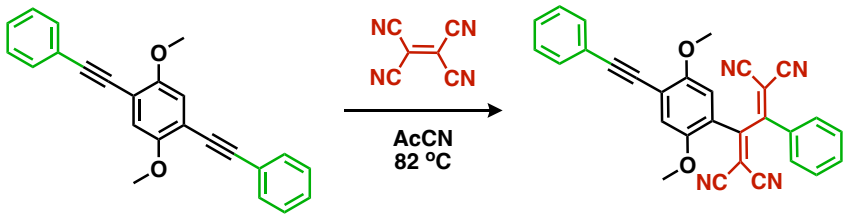

Scheme 6. [2+2] CA-RE reaction of **15** with TCNE.

The reaction of alkyne **15** with TCNE yielded a product similar to that obtained from the reaction of acetylene substituted alkyne **14**. Optimized geometries for the stationary points for the formation of TCBD product **P5** are depicted in Figure 5-6 and the potential energy profile is illustrated in Figure 7. The first step of the reaction is exergonic by 20.5 kcal/mol and the overall reaction is quite exergonic by 34.3 kcal/mol with respect to **RC4**.

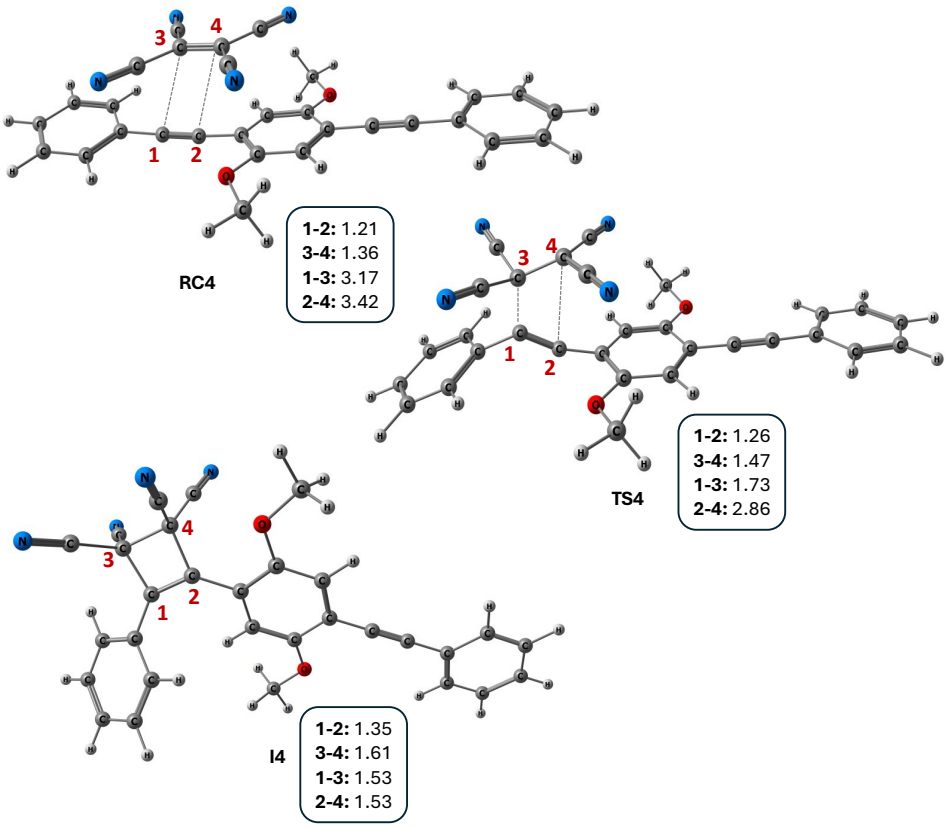

Figure 5. Optimized geometries of the stationary points **RC4**, **TS4** and **I4** at PCM/M06-2X/6-311++G(d,p)//M06-2X/6-31+G(d,p) level in acetonitrile. Distances are given in Å.

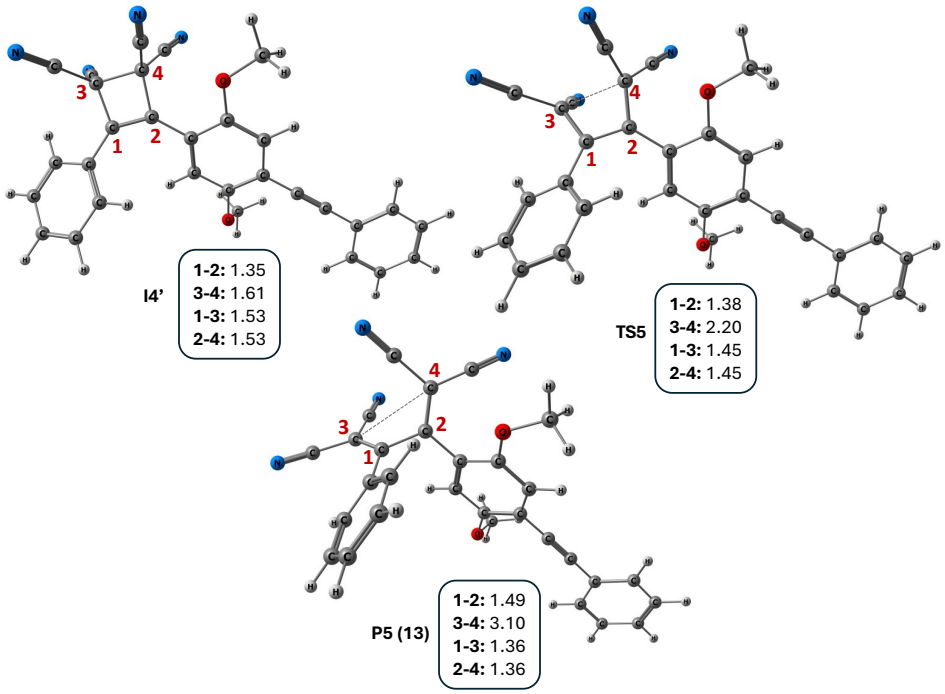

Figure 6. Optimized geometries of the stationary points **I4'**, **TS5** and **P5 (13)** at PCM/M06-2X/6-311++G(d,p)//M06-2X/6-31+G(d,p) level in acetonitrile. Distances are given in Å.

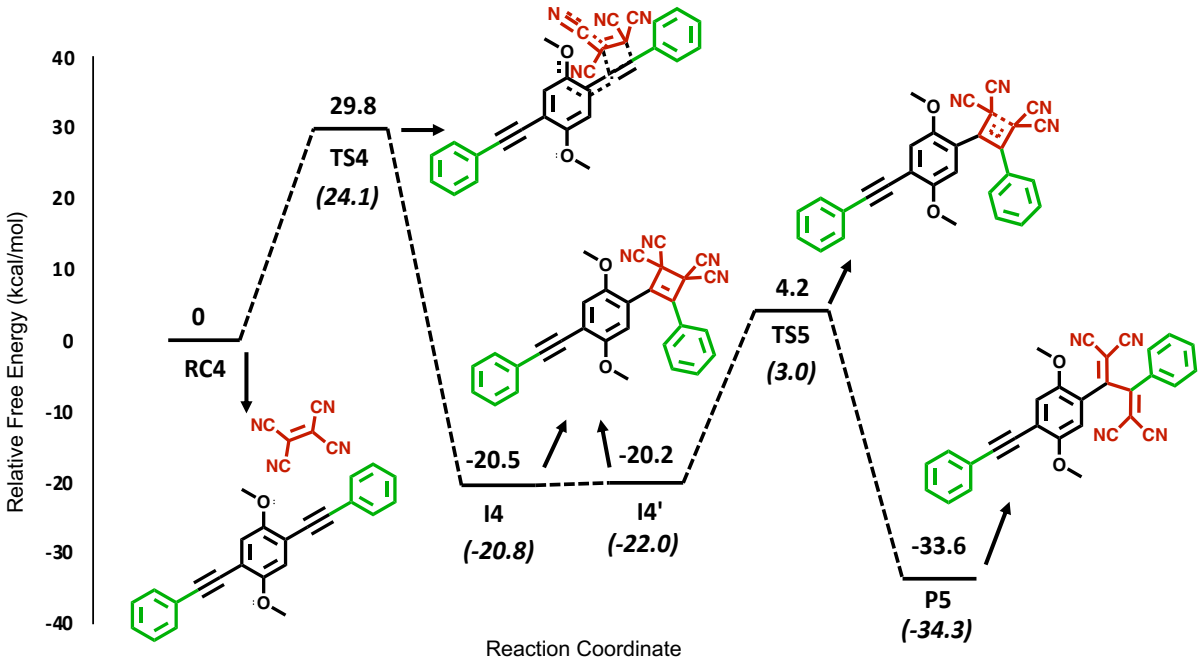

Figure 7. Potential energy profile for the formation of **P5** at PCM/M06-2X/6-311G++(d,p)//M06-2X/6-31G+(d,p) level in acetonitrile. Energy values in parenthesis are solvent energies.

2.4. Mechanistical Studies for the Formation of Intramolecular Cyclization Product 21

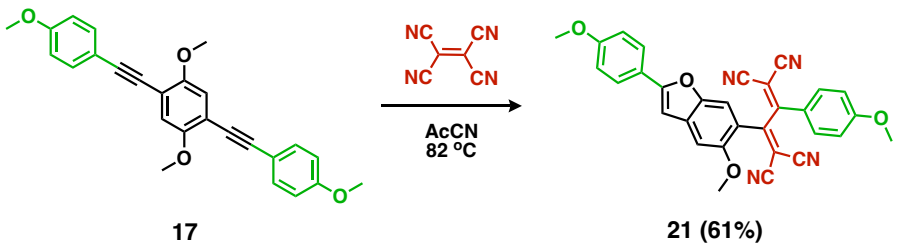

17 21 (61%)

Scheme 7. [2+2] CA-RE reaction of **17** with TCNE.

The [2+2] CA-RE reaction of methoxy-substituted alkyne **17** with TCNE yielded an unexpected cyclization product after column chromatography. Given the rarity of post-modification reactions after TCNE addition, the mechanism behind the cyclization was investigated in detail.

To begin examining the mechanism for the formation of **21**, a series of experimental studies were conducted. We were not sure whether TCNE was adding to **17** first followed by cyclization, or if cyclization occurred first and then TCNE was added. Table 1 outlines the different addition sequences which were analyzed.

Table 1. Reaction condition analysis for formation of **21**.

1	**Alkyne 17**	**-**	**-**	✗
2	**Alkyne 17**	**TCNE**	**-**	✗
3	**Alkyne 17**	**TCNE**	**SiO_2**	✓

In the first entry, only alkyne **17** was stirred at 82 °C in acetonitrile and no cyclization product was observed. In the second entry, the alkyne **17** was added first, followed by TCNE, and the reaction was stirred at 82°C in acetonitrile. Crude ^{1}H NMR analysis revealed that there was no cyclization product, and alkyne did not react with TCNE. In the third entry, the alkyne was added first, followed by TCNE, and finally SiO_2 was added. The reaction mixture was stirred in acetonitrile at 85 °C. After purification, the main product observed was the cyclization product, with a minor amount of mono TCNE addition product present. This led us to conclude that TCNE was first added to the molecule, followed by cyclization. After this experimental observation, we proposed the reaction mechanism shown in Scheme 8.

The initial two steps for the formation of **I7** are common to all pathways proposed. (see section 2.1 Scheme 4). After TCNE is added to the molecule (Scheme 8), intramolecular cyclization occurs. A three-step reaction mechanism has been proposed for the formation of the cyclization product **PC10**. The third step starts with the resonance structure of **I7'**and the abstraction of proton from silica through **TS8**. Second step involves the nucleophilic of negatively charged oxygen onto the carbon on the allene forming intermediate **I9**. The corresponding barrier was

calculated to be 16.3 kcal/mol relative to initial reactant complex **RC5**. In the final step, silica anion (which is formed after **TS8**) abstracts methyl from **I9**, producing cyclization product **PC10**.

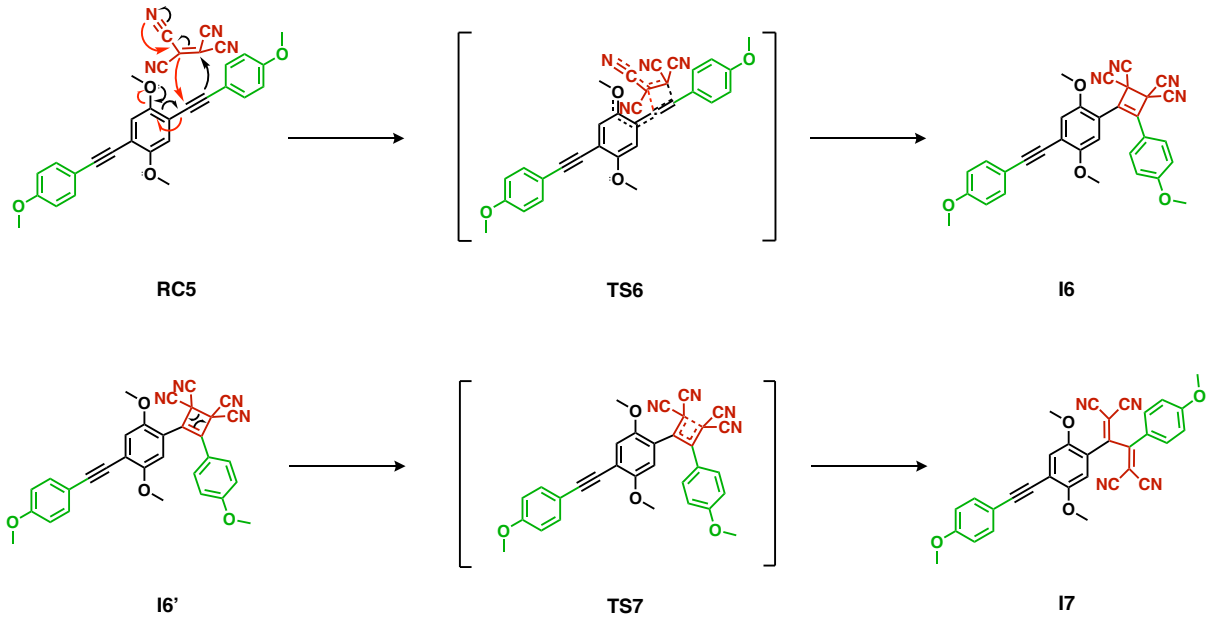

Scheme 8. Proposed mechanism for cyclization product **P10**.

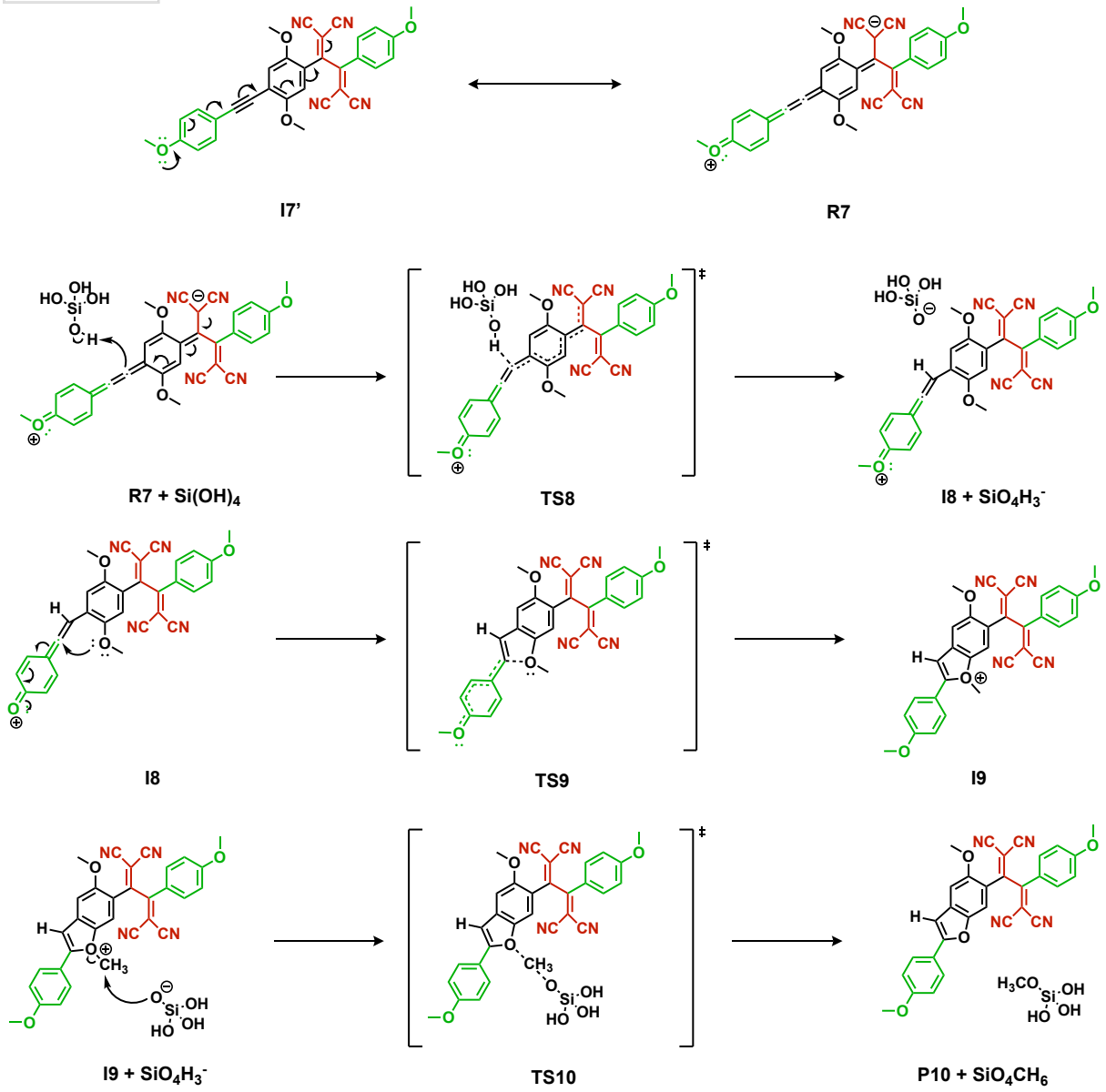

Scheme 8 (continues). Proposed mechanism for cyclization product **P10**.

The optimized geometries are illustrated in Figure 8-12. Formation of the cyclization product **P10** is both exergonic that strongly drives the potential energy profiles downhill. The overall energy profile is given in Figure 13.

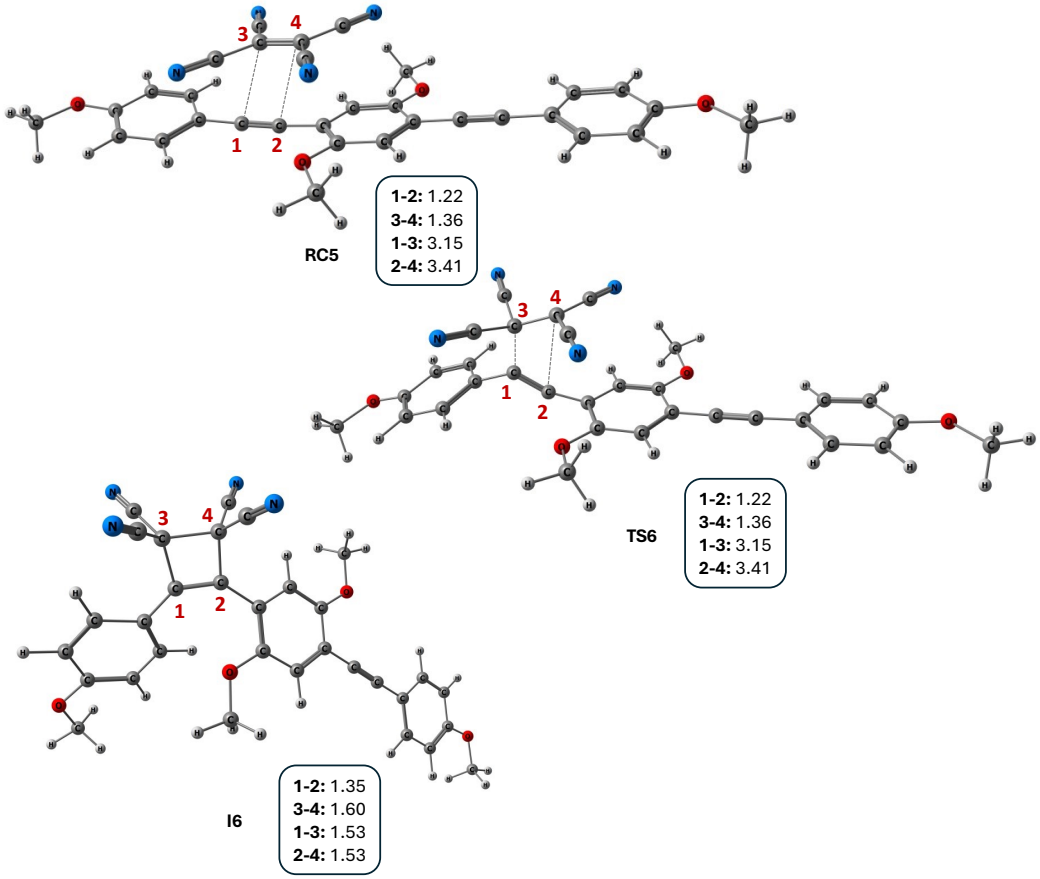

Figure 8. Optimized geometries of the stationary points **RC5**, **TS5** and **I6** at PCM/M06-2X/6-311++G(d,p)//M06-2X/6-31+G(d,p) level in acetonitrile. Distances are given in Å.

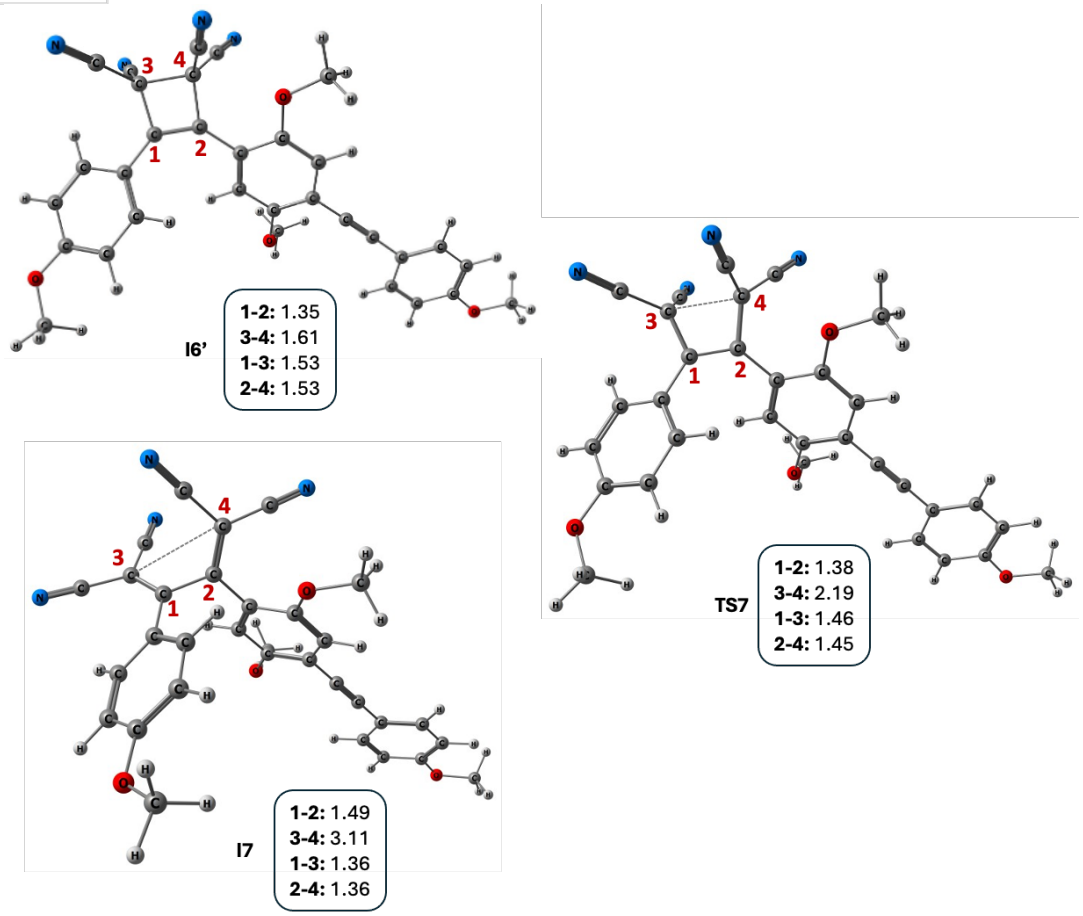

Figure 9. Optimized geometries of the stationary points **I6'**, **TS7** and **I7** at PCM/M06-2X/6-311++G(d,p)//M06-2X/6-31+G(d,p) level in acetonitrile. Distances are given in Å.

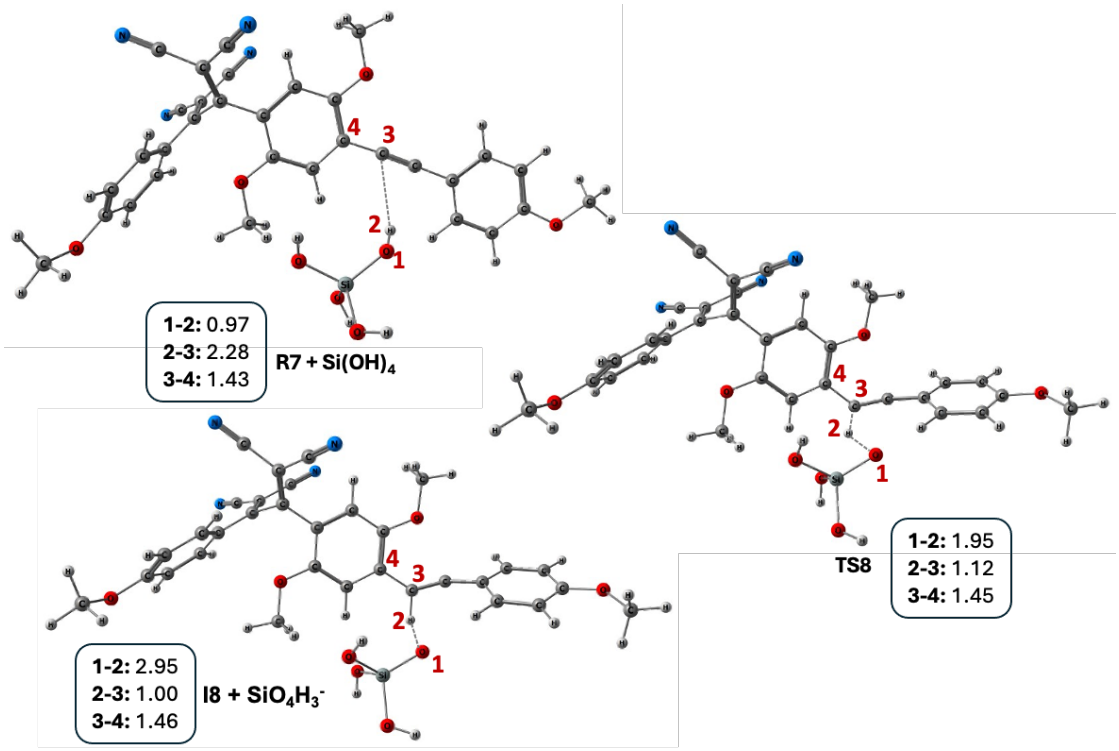

Figure 10. Optimized geometries of the stationary points **R7 + Si(OH)$_4$**, **TS8** and **I8 + SiO$_4$H$_3^-$** at PCM/M06-2X/6-311++G(d,p)//M06-2X/6-31+G(d,p) level in acetonitrile. Distances are given in Å.

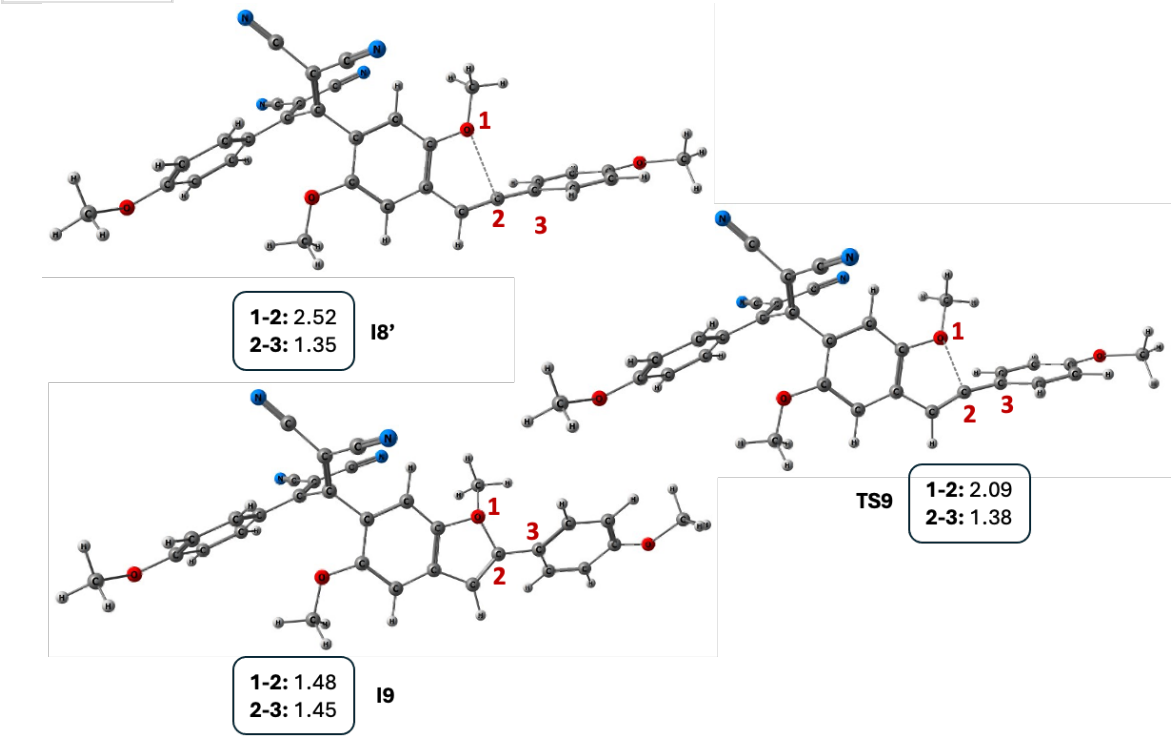

Figure 11. Optimized geometries of the stationary points **I8'**, **TS9** and **I9** at PCM/M06-2X/6-311++G(d,p)//M06-2X/6-31+G(d,p) level in acetonitrile. Distances are given in Å.

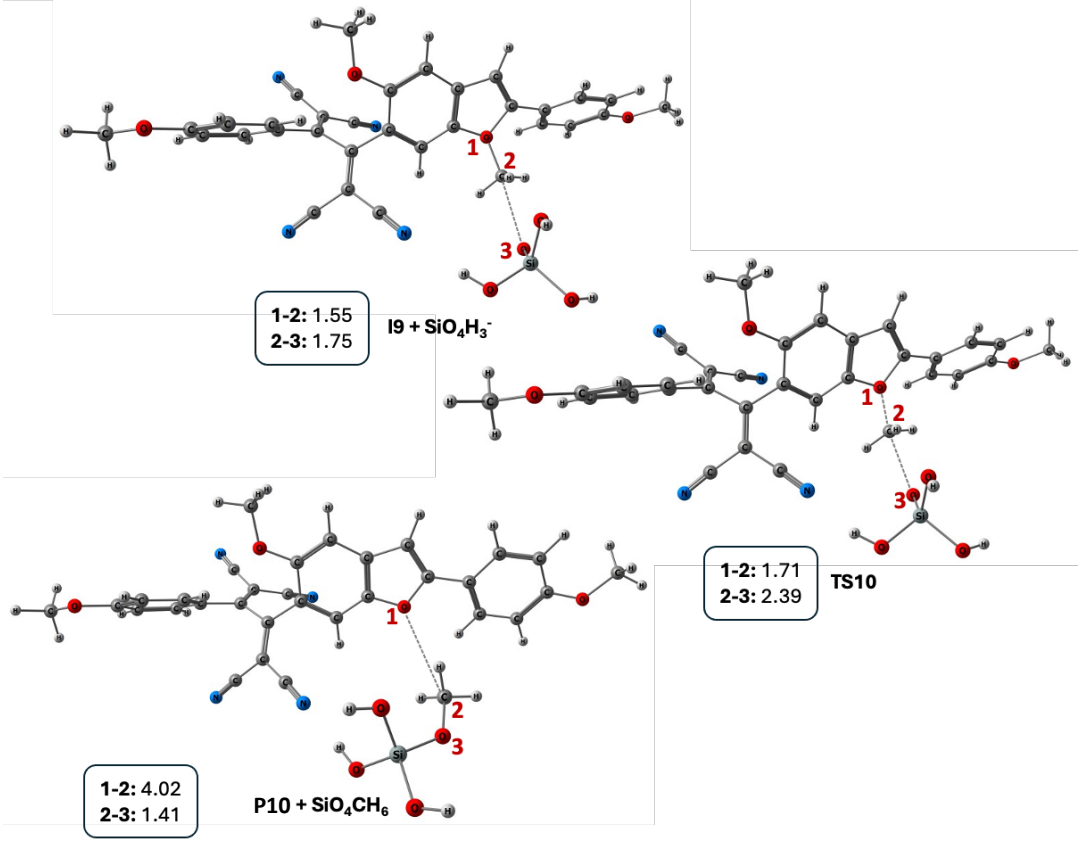

Figure 12. Optimized geometries of the stationary points **I9** + **$SiO_4H_3^-$**, **TS10** and **P10** + **SiO_4CH_6** at PCM/M06-2X/6-311++G(d,p)//HF/6-31+G(d,p) level in acetonitrile. Distances are given in Å

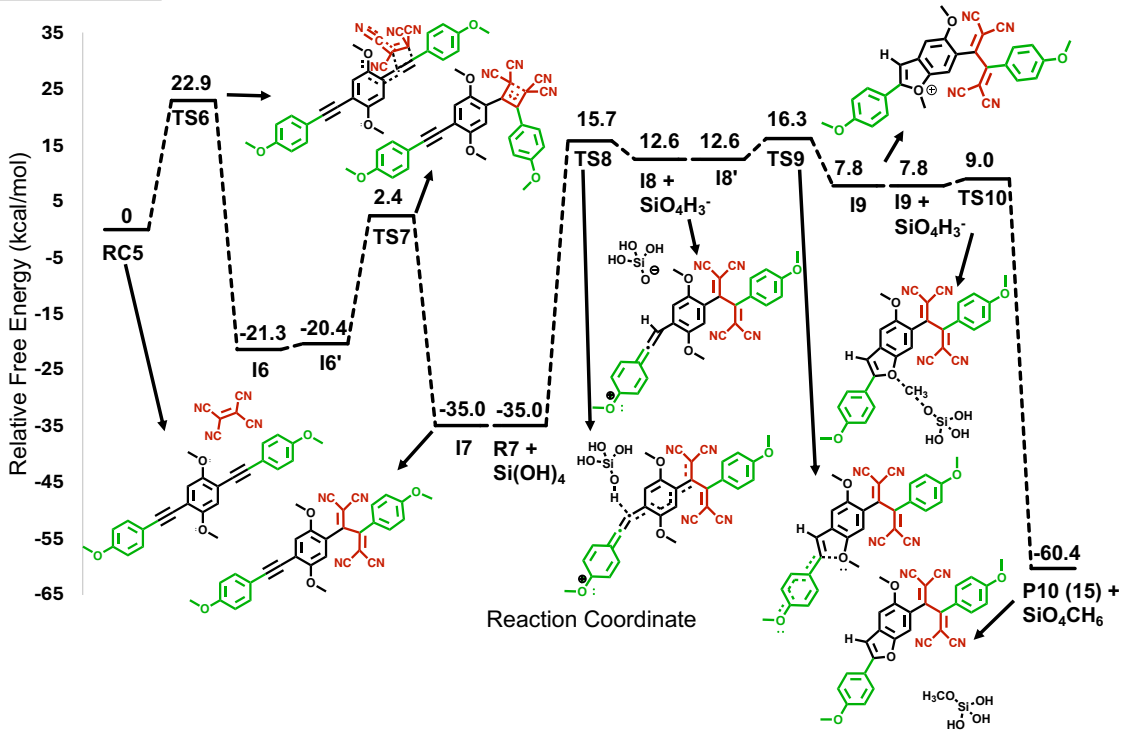

Figure 13. Potential energy profile for the formation of **P10** at PCM/M06-2X/6-311G++(d,p)//M06-2X/6-31G+(d,p) level in acetonitrile and PCM/M06-2X/6-311G++(d,p)//HF/6-31G+(d,p) for **I9 + $SiO_4H_3^-$**, **TS10** and **P10 + SiO_4CH_6**. Energy values are solvent energies. The energy values were aligned to the same scale by taking the energy values of the previous steps' intermediate and adding the energy value of the leading transition state.

2.5. [2+2] CA-RE Reaction of *N,N*-Diethylaniline Substituted Alkyne (16)

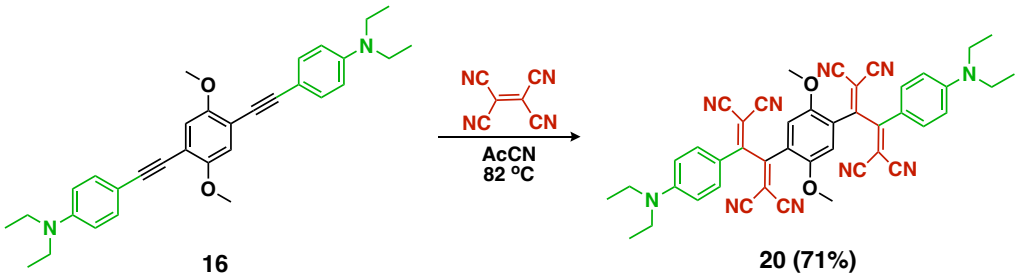

Scheme 9. [2+2] CA-RE reaction of **16** with TCNE.

N,N-diethylaniline substituted alkyne **16** reacted with TCNE from both alkyne moieties unlike alkynes **14** and **15**, which reacted from only one alkyne moiety. This result was anticipated due to strong electron donating ability of *N,N*-diethylaniline unit.[8] The examples of di-addition of TCNE to both alkyne moieties were reported previously by Dengiz's group as well.[9] Therefore, we did not perform any energy calculations regarding the [2+2] CA-RE reaction of **16** with TCNE.

3. Results and Achievements

In this study, the addition of TCNE to various symmetrical alkynes (**14-17**) was analyzed mechanistically, and the potential energy profiles along the reaction pathways were investigated by means of DFT calculations. It is important to note that the type of the alkynes used determines the nature of the products. The isolated TCNE addition and cyclization products can be seen in Figure 17.

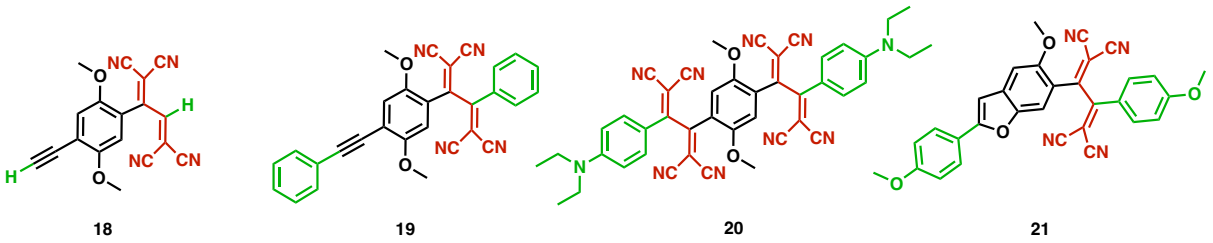

Figure 14. TCBD products **18-21**.

Initially, a three-step reaction mechanism is proposed for the [2+2] CA-RE reaction. However, our calculations demonstrated that the formation of cyclobutene intermediate occurs via an asynchronous-concerted pathway followed by retro electro cyclization. For alkyne **16**, di-addition was expected due to strong electron donor behavior of *N,N*-diethylaniline substituent; consequently, it's energy profile was not examined. The most notable outcome was observed with the methoxy substituted alkyne **17**. After TCNE addition, a post-modification reaction led to cyclization product **21**. The potential energy profile for the formation of **21** is downhill with respect to the **RC5,** and thus the proposed mechanism appears to be plausible.

4. HPC Benefits

This PoC study enabled the elucidation of reaction mechanisms for the formation different products obtained from CA-RE reactions using quantum chemistry calculations. Since Dengiz's research group specializes in experimental studies, they requested guidance from an academic and infrastructure expert experienced in the field of computational organic chemistry to rationalize the experimental observations. In this PoC study, a master's student who had only conducted experimental studies and had never used computational chemistry tools or HPC before received mentorship in computational organic chemistry field from an HPC expert at NCC Türkiye. As a result of this mentorship and the PoC study, the student is able to model the mechanisms of organic reactions on the national HPC infrastructure TRUBA using Gaussian software package. The master's student also plans to continue working on computational organic chemistry in her PhD studies. As a result of this study, it is also planned to publish an article in an academic journal indexed by SCI.

5. Challenges

For researchers who has never used a terminal or is unfamiliar with Linux commands and new to the field of computational chemistry, optimizing stationary points especially transition states and submitting jobs on an HPC system can be quite challenging. Furthermore, the computations

can take a long time depending on factors such as the selected method and basis set, or the size of the molecule.

To address these challenges, the master student initially performed the calculations using the semi-empirical PM6 method, which requires relatively shorter computation times, on a local computer. As the student conducted numerous calculations on the local computer, she became more proficient with the software and began to achieve success in optimizing geometries of the structures. At this point, the calculations were transferred to the HPC systems using DFT methods and higher-level basis sets. Thanks to this step-by-step approach, the student eventually gained proficiency in both using the software and submitting jobs on the HPC infrastructure.

6. References

[1] Donckele, E. J., Finke, A. D., Ruhlmann, L., Boudon, C., Trapp, N., & Diederich, F. *Organic Letters*, **2015**, *17*(14), 3506–3509. DOI: 10.1021/acs.orglett.5b01598.

[2] Bruce, M. I., Rodgers, J. R., Snow, M. R., & Swincer, A. G. *J. Chem. Soc., Chem. Commun.*, **1981**, (6), 271–272. DOI: 10.1039/c39810000271.

[3] Michinobu, T.; May, J. C.; Lim, J. H.; Boudon, C.; Gisselbrecht, J.-P.; Seiler, P.; Gross, M.; Biaggio, I.; Diederich, F. *Chem.Comm.,* **2005**, 737–739. DOI: 10.1039/b417393g.

[4] Hoffmann R.; Woodward R. B.. *J. Am. Chem. Soc.,* **1965**, *87* (9), 2046–2048. DOI: 10.1021/ja01087a034.

[5] Michinobu, T.; May, J. C.; Lim, J. H.; Boudon, C.; Gisselbrecht, J.-P.; Seiler, P.; Gross, M.; Biaggio, I.; Diederich, F. *Chem.Comm.,* **2005**, 737–739. DOI: 10.1039/b417393g.

[6] Kivala, M.; Boudon, C.; Gisselbrecht, J.-P.; Seiler, P.; Gross, M.; Diederich, F. *Chem Comm*., **2007**, 4731–4733. DOI: 10.1039/B713683H.

[7] Hansen, J. K.; Tortzen, C. G.; Sørensen, P. G.; Brøndsted Nielsen, M. *Chemistry – A European Journal* **2022**, *29* (3). DOI:10.1002/chem.202202833.

[8] Michinobu, T.; Diederich, F. *Angewandte Chemie International Edition* **2018**, *57* (14), 3552–3577. DOI:10.1002/anie.201711605

[9] Mammadova, F.; Inyurt, F. C.; Barsella, A.; Dengiz, **2023**, *209*, 110894. DOI:10.1016/j.dyepig.2022.110894.